一般社団法人　電子情報通信学会
THE INSTITUTE OF ELECTRONICS,
INFORMATION AND COMMUNICATION ENGINEERS

信学技報
IEICE Technical Report
A・P2022-179(2023-01)

Integrated transition with dielectric rod for vacuum chamber

Derek GRAY,　Julien Le KERNEC and Konstantinos KONTIS

James Watt School of Engineering,　University of Glasgow,　Glasgow,　UK
E-mail:　(Derek.Gray,　Julien.LeKernec,　Kostas.Kontis) @glasgow.ac.uk

Abstract　Conducting monostatic and bistatic radar and propagation measurements across 33 to 75GHz within a vacuum chamber under Mars atmospheric pressure or Moon vacuum while a thruster erodes regolith and rock simulant present a number of difficulties.　Passing through the boron glass windows incurred 3dB loss showing the need for a proper low loss *mm*-wave transition.　Such a transition from an external air filled waveguide to an antenna inside the chamber must hold the 101.3kPa to 535Pa or 0Pa pressure difference.　A single-piece cross-linked polystyrene filled rectangular waveguide transition to a dielectric rod looks promising to deliver 18 to 21dBi Gain across an octave.

Key words　polyrod antenna,　horn antenna,　radio propagation,　Moon regolith.

1. Introduction

Thrustered soft landings on the Moon and Mars throw up loose regolith and small stones which obscures view of the surface blocking accurate altitude measurement by laser range finding.　The Moon is airless with a thin diurnal dependent plasma sheath and does not have an active atmosphere with rapid gas pressure changes, biological processes affected surfaces nor blowing dust. Thus blockage of view of the surface can only be caused by the thruster-surface interaction ejecta.　The amount and type of ejecta cannot be predicted without a site inspection prior to landing,　so it is assumed that a worst case will always occur causing a laser altimeter to fail in the final and critical minute of a landing.　Thus a radio altimeter that can accurately measure the distance to the surface through an ejecta cloud appears to be the only option.

The vacuum chamber at University of Glasgow can achieve and hold a vacuum and at 2.5m diameter is large enough to facilitate modest-sized experiments to study Moon and Mars surface-thruster interaction,　Figure 1. A thruster simulator is aimed at a tray of regolith simulant held about 0.4m above the chamber floor.　The chamber has 28 off DN 200 ISO-K ports which allow for observation of a trial or passing cables to instruments inside the chamber.　At present,　N_2 gas at 600°C with velocity of Mach 6.6 passing through a 0.5mm nozzle is used to simulate a hydrazine thruster under Lunar conditions. The Lunar regolith simulant used are commercially available glass bubbles which do not cake nor absorb moisture,　are easy to clean up and safe to handle [1]. Type K1 which has a density of 0.125g/cc and an effective top size of 120μm,　and type K46 which has a density of 0.46g/cc and an effective top size of 80μm are being used [1].

Figure 1:　Photograph of the vacuum chamber,　with Mr. Elsayed for scale.

As the regolith simulant target size and position within the chamber are not yet fixed,　the dependent look angle

and the diameters of the footprint and glistening zones are unknown at the time of writing. However, the aim is to be able to conduct 3 types of propagation measurement within the chamber:

- *transmission*: direct window to opposing window to measure effects of a cloud of ejecta and/or the N_2 jet.
- *bistatic*: Tx and Rx antennas in opposing windows aimed at the regolith target tray to measure reflection as the surface erodes.
- *monostatic*: Tx and Rx antennas in the same window aimed at the regolith target tray to measure reflection as the surface erodes, akin to a fielded radio altimeter.

The frequency band of interest is 33 to 75GHz, dictating the use of WR-22 and WR-15 waveguides. The use of X-band is considered a safe fallback as the ejecta particles are much smaller than a wavelength but a larger form factor is disadvantageous for space missions.

Figure 2: Rx side spectrum analyzer with WR-22 transition held outside a DN200 ISO-K port on right.

2. Initial *mm*-wave transmission measurement.

Pairs of commercially available V 1.85mm coaxial to WR-22 and WR-15 transitions were used as antennas for "external transmission" tests across the vacuum chamber between a pair of facing boron glass windows. The Tx side transition was held 4cm off its window, while the Rx side was 9cm off its window, Figure 2. The UG385 or UG383 flange face to flange face separation was ~2.7m. The measured loss at 35GHz was 57dB been 15dB less than the theoretical free space loss of 72dB, which suggests that the Gain of each coax to WR-22 transition was 7.5dBi. This Gain value is a little lower than expected, so there appears to be up to 3dB loss over free space from transmitting through the chamber. Note that alignment was difficult as seen in the 1.5dB difference in <0s data from consecutive days in Figure 3.

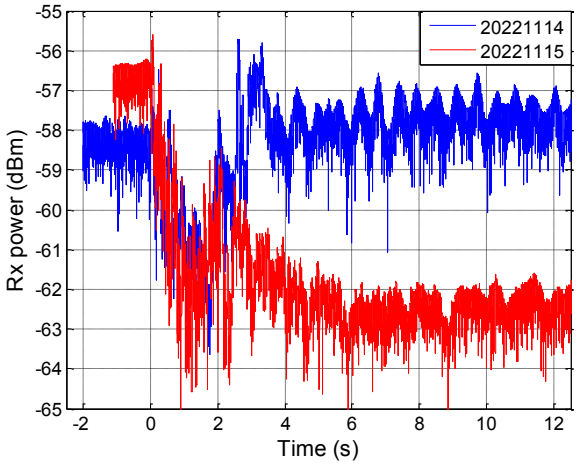

Figure 3: Effect of N_2 jet firing at 0s on received power at 35GHz from 2 consecutive tests.

There were many unexpected features in the measured data. The 0.5Hz dominant oscillation in Figure 3 shows that the transitions were vibrating. This is likely from a pump and will be traced. The attenuation effect in the first 2.2s after firing is remarkably consistent, and was not expected. Further, after 2.2s the signal level either returned to baseline or -5.5dB below the baseline. The cause of these phenomena is unknown at present.

Reducing the distance between the antennas will decrease the free space loss, but necessitates moving inside the chamber. The vacuum seal must be maintained, but it is understood that commercially available waveguide pressure windows are narrowband, where at least octave performance is wanted so as to gather as much data as possible from each thruster firing to minimize running costs. In-house low-cost manufacture of transitions integrated directly with the antennas would be preferred. It was assumed that a circular hole through a steel ISO200-K blanking flange will minimize stress and be the easiest to seal. For the antennas themselves, the design priorities for any antennas placed within the chamber must have ease of

inspection for contamination and ease of cleaning. Thus the aim of this work is to prepare transition-antenna designs that will be submitted for review by the vacuum engineers at the chamber manufacturer whose comments will be incorporated into the next design iteration. The first pass designs presented here were for X-band.

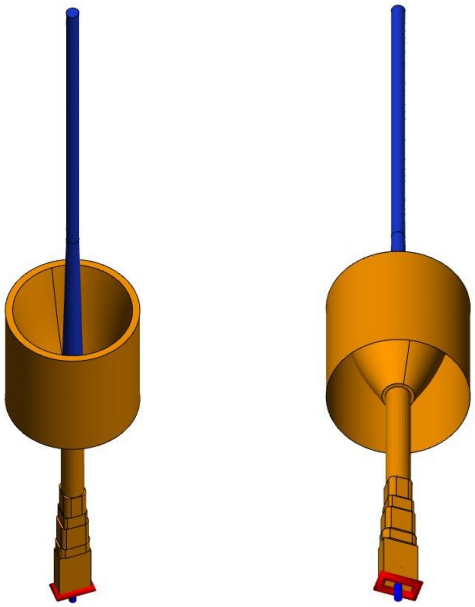

Figure 4: Stripped CAD of polyrod antenna with 4-step transition, from FEKO™.

3. Polyrod antenna with 4-step transition

Travelling wave waveguide0fed polystyrene (ε_r=2.54) rod "polyrod" was invented about 100 years ago [2]. Optimized designs consisting of polystyrene filled waveguide to polystyrene cone to polystyrene cylinder are described in [3]. This simple geometry is suited to automated optimization by the built-in utilities in any commercially available antenna simulator to give ~19dBi across most of an octave. Using a conductive cup around the base of the polyrod cone will further increase the Gain to ~22dBi [4]. Such a simple rotationally symmetric cup is also amenable to automated optimization and will isolate the polyrod from the ISO200-K blanking flange that it projects through. With the diameter of polystyrene filled circular waveguide fixed at 16mm and a 2.5mm wide ring at the base of the cup, the GA optimizer in FEKO™ produced a 167mm tall cone feeding a 237mm tall 8.9mm diameter cylinder inside a 92mm tall cup having 81mm mouth, Figures 4 and 5. Total scaled polyrod length will be 100mm for WR-22 and 67mm for WR-15.

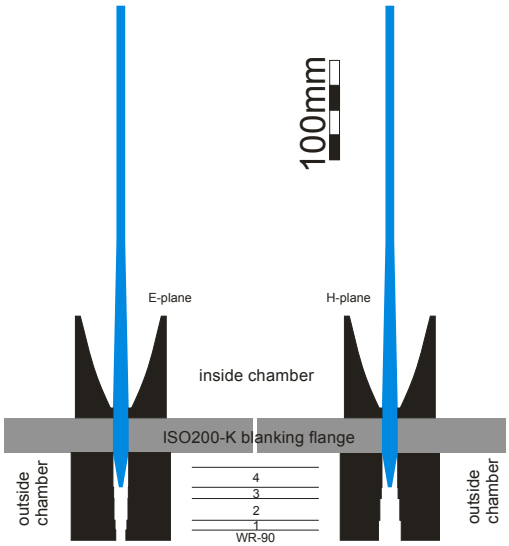

Figure 5: Cross-sections of polyrod antenna with 4-step transition from WR-90 to 16mm circular waveguide.

TABLE 1: 4-step X-band transition dimensions.

Section	E-plane (mm)	H-plane (mm)	length (mm)
WR-90	10.16	22.86	∞
1	12	22.86	10.1
2	14	20	21.6
3	15	17	11.5
4	16	16	20.2

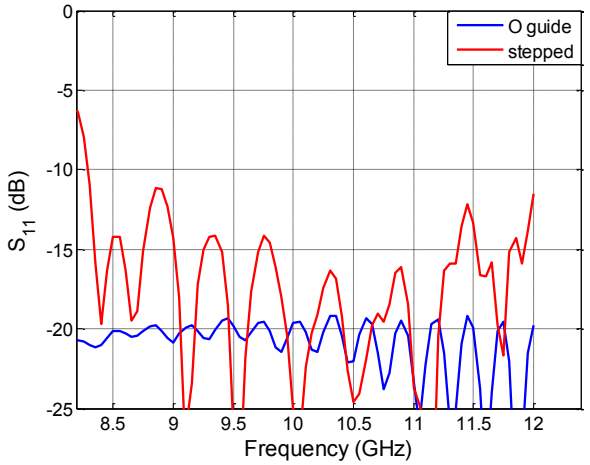

Figure 6: Simulated S_{11} of polyrod antenna, from FEKO™.

A 4-step transition from to WR-90 to a polystyrene filled 16mm diameter circular waveguide inspired by [5] was also optimized using the GA in FEKO™, Figures 4 and 5 and Table 1. A 35mm long cone projected into the 4th step to transition from air-filled to polystyrene filled waveguide. It is expected that a bulge with a thin gasket will be added

between the outside transition and the ISO200-K blanking flange for sealing.

Comparing the S_{11} of the polyrod with and without the 4-step with matching cone showed that the transition introduced numerous resonances, Figure 6. Most of the minor discontinuities introduced into the Directivity align with the higher S_{11} resonances, Figure 7. A peak of 21dBi was achieved at 10.8GHz. The close to linear frequency characteristics before and after the Directivity peak are attractive for this application.

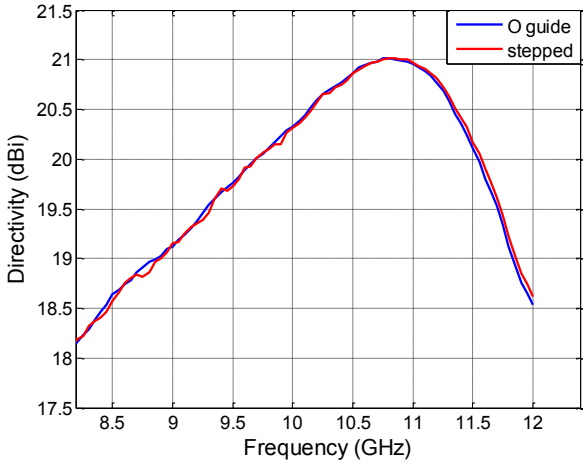

Figure 7: Simulated directivity of X-band polyrod antenna, from FEKO™.

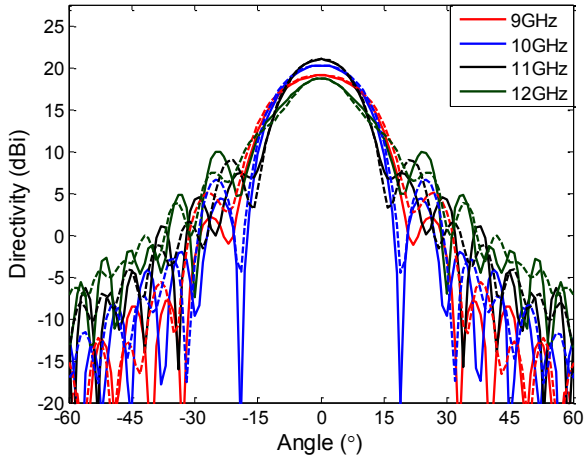

Figure 8: Far field radiation patterns of polyrod antenna, – E-plane, -- H-plane, from FEKO™.

The E and H-plane radiation pattern shapes changed gradually across X-band, Figure 8. The 3dB beamwidths ranged from ~25° to 15° with the H-plane generally broader than the E-plane, Figure 9. Equalization occurred at 11.4GHz. Compared to an aperture antenna, the first sidelobe levels were relatively high ranging between -15dB and -10dB, as would be expected for any travelling wave antenna [6].

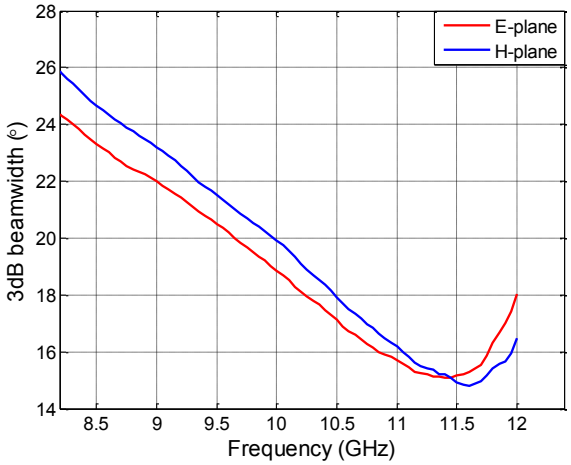

Figure 9: 3dB beamwidths of polyrod antenna, from FEKO™.

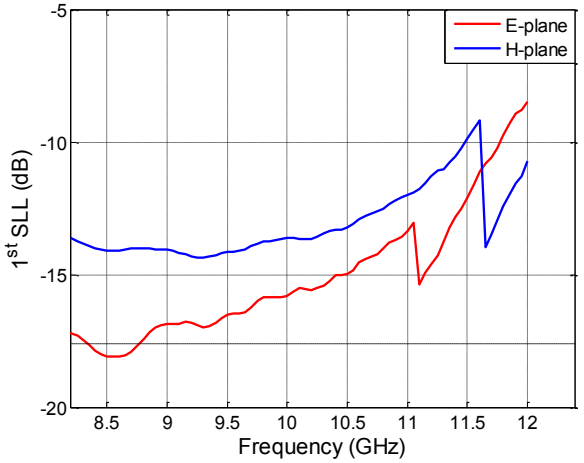

Figure 10: First sidelobe levels of polyrod antenna, from FEKO™.

4. First pass X-band horn designs

The polyrod with cup geometry is not compatible with simple mechanical steering, whereas a horn with a swiveling ball joint feed can steer across ±45°. A wall thickness of 20mm was arbitrarily chosen for X-band, which will scale to 5mm for WR-22 and 3.3mm for WR-15. It was presumed that such thick-walled horns would tolerate any shockwaves within the chamber and have a considerable thermal mass. These first pass designs were fed directly by WR-90.

The baseline design was a pyramidal horn 555mm long with a 267x217mm mouth, Figure 11. The preferred design was a smooth-walled spline circular horn based on

[7] having a 212mm diameter mouth which would scale to 53mm for WR-22 and 35mm for WR-15, which will be manufactured in-house. The length of the spline horn came out as 430mm, which would scale to 107mm for WR-22 and 71mm for WR-15. The X-band spline horn was 120mm shorter than the pyramidal horn.

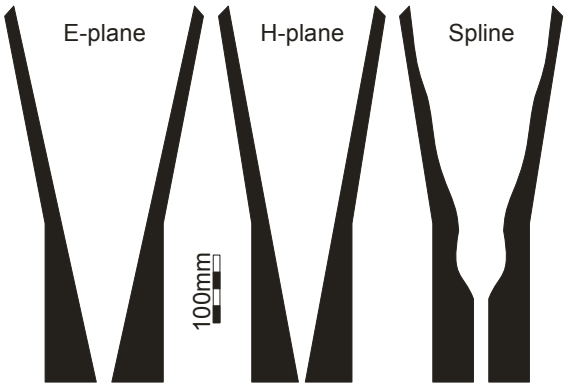

Figure 11: Silhouettes of first pass X-band pyramidal and spline designs fed by WR-90 waveguide, to scale.

Both horns were well matched across X-band, Figure 12. The pyramidal horn had a consistent S_{11} oscillation across the entire band from the neck discontinuity. Worryingly, there was a 0.2dB ripple in the Directivity of the pyramidal horn which likely disqualifies it from the present scientific measurement application, Figure 13. In contrast, the results to date for the spline horn show a smooth Directivity characteristic and 1.5dB higher peak Directivity despite having a smaller aperture. Thus the superiority of a managed aperture has been demonstrated for the 25dBi medium Gain class of antenna, even in this crude initial prototype design.

The radiation patterns of the pyramidal horn matched expectations in that the E-plane had high sidelobes and the H-plane was like a Gaussian distribution, Figure 14. Ripple appeared in both the 3dB beamwidths and E-plane first sidelobe level of the pyramidal horn as a result of the TM standing waves within the horn. The spline horn did not produce a rotationally symmetric radiation pattern as was hoped, Figure 15. More effort needs to be put into managing the modes with this horn. Interestingly, the 3dB beamwidths were close to equal for most of the band whereas the 10dB beamwidths and first sidelobe levels were not, Figures 15 to 17. This suggests that there was management of most of the power and the center of the aperture in this first crude attempt at a spline horn.

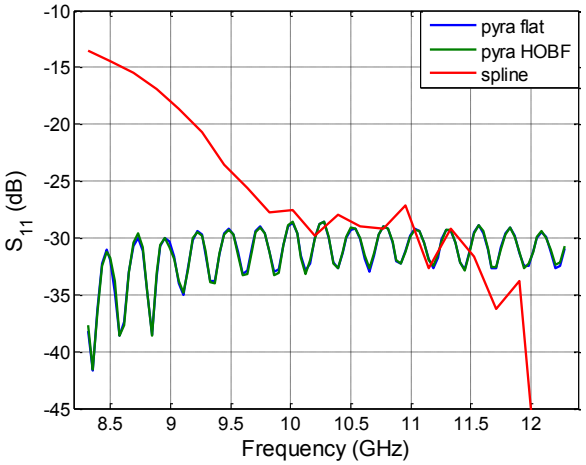

Figure 12: Simulated S_{11} of X-band horns; from FEKO™.

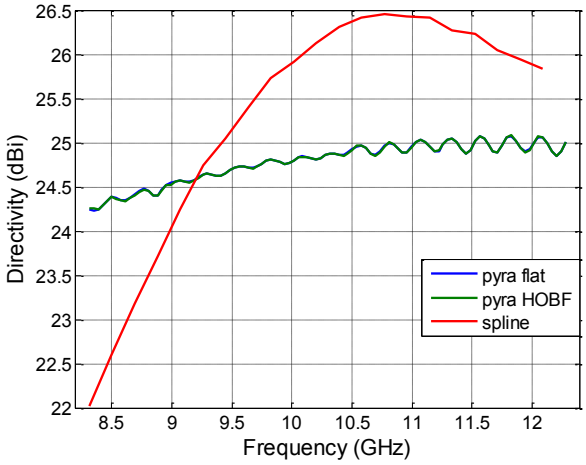

Figure 13: Simulated directivity performance of pyramidal and spline horns; from FEKO™.

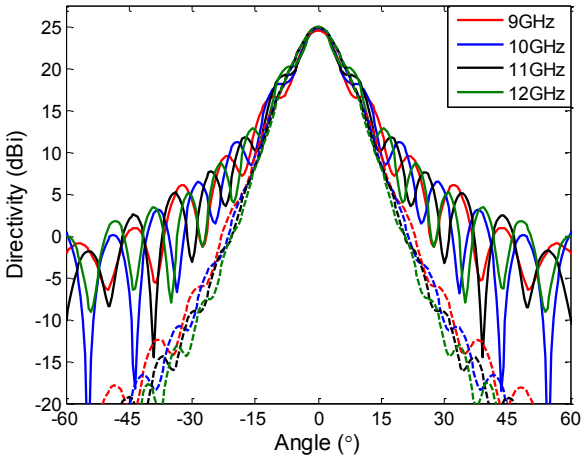

Figure 14: Far field radiation patterns of pyramidal horn; – E-plane, -- H-plane, from FEKO™.

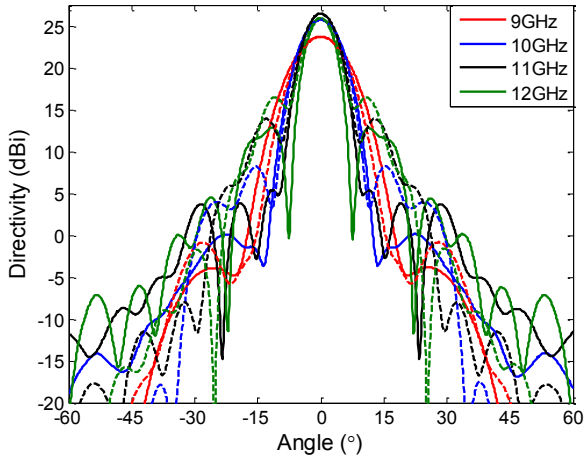

Figure 15: Far field radiation patterns of spline horn; – E-plane, -- H-plane, from FEKO™.

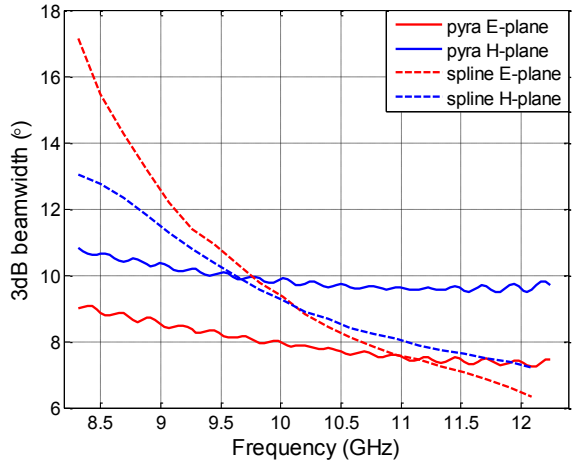

Figure 16: 3dB beamwidths of horns; from FEKO™.

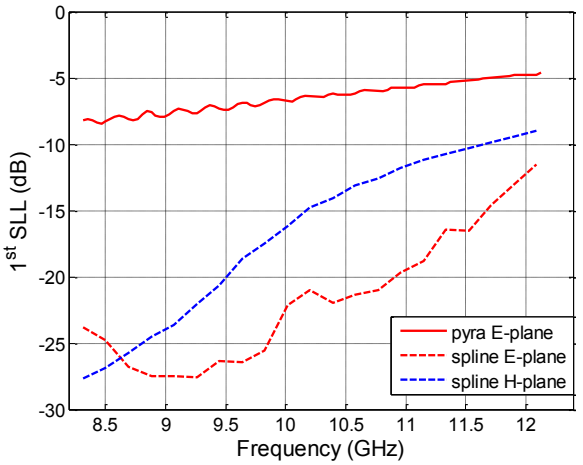

Figure 17: First sidelobe levels of horns; from FEKO™.

5. Conclusions and future work

A program to develop antennas for use within a vacuum chamber to measure the propagation effects of thruster surface interaction was started. The initial designs for low-medium Gain polyrod with a cup and a spline horn antenna look promising in that both are well matched and gave acceptable radiation pattern performance. Further work on both types will be contingent on the creation of a sealed polystyrene filled waveguide transition through an ISO200-K blanking flange.

Acknowledgement

The authors thank Mr M. Elsayed and Mr S. Subramanian for conducting the vacuum chamber experiments and assisting with the *mm*-wave measurements. This work could not have been done without a FEKO™ 2022 trial. The authors wish to thank Ms. H. Hunter-Hill of Altair UK for arranging that trial.

The primary author is greatly indebted to Dr C. Granet and Dr. J. Kot for the comprehensive discussions on analysis of pyramidal horns and the design philosophy of spline horns. Likewise to Dr. H. Suzuki of CSIRO for fruitful discussions on propagation measurements.

8. References

[1] "3M™ Glass Bubbles, K Series, S Series," 3M Oil & Gas, 2009.

[2] G.C. Southworth, "Short wave radio system," United States patent 2,206,923, granted July 9th, 1940.

[3] G.C. Southworth, *Principals and applications of waveguide transmission*, D. van Nostrand Company, Inc., Princeton, NJ, 1950.

[4] K. Sato, I. Oshima & H. Nakano, "Rod antenna for 28-GHz band operation," IEEE-APS Topical Conference on Antennas and Propagation in Wireless Communications, 2022.

[5] R. Béhé, "Dispositif de couplage d'un guide d'onde circulaire à un réflecteur parabolique de révolution," French patent 2,096,684, granted June 3rd, 1970.

[6] K.M. Keen, "On the equivalent aperture formation of an endfire array," IEEE Trans Antennas Propag., pp 831-832, Nov. 1974.

[7] C. Granet, G.L. James, R. Bolton & G. Moorey, "A smooth-walled spline-profile hom as an alternative to the corrugated horn for wide band millimeter-wave applications," IEEE Trans Antennas Propag., Vol. 52, No 3, March 2004, pp. 848-854.